

## Ternary hypervalent silicon hydrides via lithium at high pressure

Tianxiao Liang,<sup>1</sup> Zihan Zhang,<sup>1</sup> Xiaolei Feng,<sup>2,3,\*</sup> Haojun Jia<sup>④</sup>,<sup>4</sup> Chris J. Pickard,<sup>5,6</sup> Simon A. T. Redfern<sup>⑤</sup>,<sup>7,8</sup> and Defang Duan<sup>⑥</sup>,<sup>1,†</sup><sup>1</sup>College of Physics, Jilin University, Changchun 130012, China<sup>2</sup>Institute for Disaster Management and Reconstruction, Sichuan University - the Hong Kong Polytechnic University, Chengdu 610207, China<sup>3</sup>Department of Earth Science, University of Cambridge, Downing Site, Cambridge CB2 3EQ, United Kingdom<sup>4</sup>Department of Chemistry, Massachusetts Institute of Technology, Cambridge, Massachusetts 02139, USA<sup>5</sup>Department of Materials Science & Metallurgy, University of Cambridge, 27 Charles Babbage Road, Cambridge CB3 0FS, United Kingdom<sup>6</sup>Advanced Institute for Materials Research, Tohoku University, 2-1-1 Katahira, Aoba, Sendai 980-8577, Japan<sup>7</sup>Asian School of the Environment, Nanyang Technological University, Singapore 639798<sup>8</sup>Center for High Pressure Science and Technology Advanced Research, Beijing 100094, China

(Received 14 September 2020; accepted 4 November 2020; published 18 November 2020)

Hydrogen is rarely observed as a ligand in hypervalent species, however, we find that high-pressure hydrogenation may stabilize hypervalent hydrogen-rich materials. Focusing on ternary silicon hydrides via lithium doping, we find anions composed of hypervalent silicon with H ligands formed under high pressure. Our results reveal two different hypervalent anions: layered  $\text{SiH}_5^-$  and tricapped triangular prismatic  $\text{SiH}_6^{2-}$ . These differ from octahedral  $\text{SiH}_6^{2-}$  described in earlier studies. In addition, there are further hydrogen-rich structures,  $\text{Li}_3\text{SiH}_{10}$  and  $\text{Li}_2\text{SiH}_{6+\delta}$ , which may be stabilized at high pressure. Our work provides pointers to future investigations on hydrogen-rich materials.

DOI: [10.1103/PhysRevMaterials.4.113607](https://doi.org/10.1103/PhysRevMaterials.4.113607)

## I. INTRODUCTION

Hypervalences are well established in chemistry, referring to aggregates, such as molecules, ions, hydrogen bonds, and other extended structures, in which main group atoms, as a result of their coordination with ligands, adopt a valence electron configuration that exceeds eight [1]. The electronegativity of hydrogen is similar to that of *p*-block element central atoms, and this explains why hydrogen is rarely observed as a ligand in hypervalent species [2]. Linear bonding in hypervalent species is visually described by the three-center-four-electron (3c-4e) model [3–5] and it is generally acknowledged that a high polarity is essential to stabilize a hypervalent bond. The Lewis-Langmuir theory of valence attributes the stability of molecules to their ability to place their valence electrons, which appropriately paired off as chemical bonds into stable octets [6,7]. This theory can be said to have survived the advent of quantum mechanics, with the electron pairs being replaced by doubly occupied molecular orbitals or approximately localized bond orbitals, and with the “cubical atom” being replaced by the directed valences of *p* bonds, so that undistorted bonds form along perpendicular axes rather than towards the corners of tetrahedra.

Some previous theoretical and experimental studies show that the alkali metal potassium (K) can form K-Si-H compounds, in which potassium silyl  $\text{KSiH}_3$  exhibits a high hydrogen content of 4.1 wt% and maintains an excellently

reversible reaction without any disproportionation through direct hydrogenation of the  $\text{KSi}$  Zintl phase near 130 °C and ambient pressure, consistent with theoretical calculations [8–11]. In 2012,  $\text{K}_2\text{SiH}_6$  with a cubic  $Fm\bar{3}m$  structure was synthesized via reactions of  $\text{K}_2\text{SiH}_6 \rightarrow 2\text{KH} + \text{Si} + 2\text{H}_2$  and  $\text{K}_2\text{SiH}_6 \rightarrow \text{K} + \text{KSi} + 3\text{H}_2$  at pressures above 4 GPa and temperatures between 450 and 650 °C. This phase contains octahedral  $\text{SiH}_6^{2-}$  and additional hypervalences of the central Si atoms [12]. We believe that there should be similar additional hypervalences for central Si atoms when combined with alkali-metal hydrides at high pressure.

In this paper, the alkali metal lithium (Li) was chosen to form Li-Si-H compounds. Here, the atomic mass of lithium is relatively light such that it enhances the hydrogen content to achieve the same stoichiometric ratio to metal as seen in  $\text{K}_2\text{SiH}_6$  and similar compounds. In addition, we explore different ternary phases and investigate their peculiar structures and properties at high pressure, and find that these potential structures may be stable at ambient pressure.

## II. COMPUTATIONAL DETAILS

Full variable-composition predictions for a Li-Si-H system were first performed within 15 000 structures using the *ab initio* random structure searching approach (AIRSS)[13,14] at pressures of 1 atm, 50 GPa, 100 GPa, and 200 GPa. Then, fixed composition predictions were employed to further search structures for stable compounds by means of the AIRSS code. The CASTEP code [15] was also used for the structure searches. The VASP (Vienna *ab initio* simulation packages) code [16] was used to optimize crystal

\*xf232@cam.ac.uk

†duandf@jlu.edu.cn

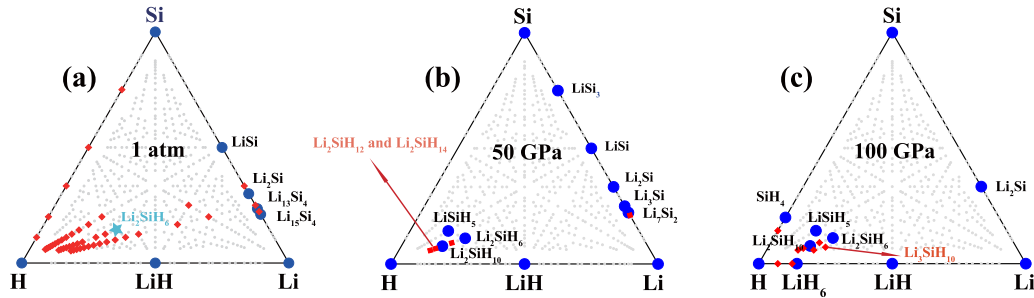


FIG. 1. The ternary phase diagram of Li-Si-H at (a) 1 atm, (b) 50 GPa, and (c) 100 GPa. Large solid blue circles represent those located on the phase diagrams, and small red diamonds represent those which did not locate on the phase diagrams. A metastable structure with a ratio of  $\text{Li}_2\text{SiH}_6$  is marked with a star in (a), which is dynamically stable.

structures and calculate the electronic properties, where the Perdew-Burke-Ernzerhof (PBE) [17] generalized gradient approximation (GGA) [18] with the projector augmented-wave method (PAW) [19] was performed. The  $1s^1$ ,  $1s^22s^1$ , and  $2s^22p^63s^23p^2$  configurations were treated as valence electrons for H, Li, and Si, respectively. The kinetic cutoff energy of 800 eV, and Monkhorst-Pack  $k$  meshes with a grid spacing of  $2\pi \times 0.03 \text{ \AA}^{-1}$  were then adopted to ensure enthalpy convergence to less than 1 meV/atom. Phonon calculations were performed in the PHONOPY code [20] to explore the dynamic stability of the proposed structures. To investigate the Si-H bonding characteristics, the integrated crystalline orbital Hamilton populations (ICOHPs) were calculated as implemented in the LOBSTER [21] package, which provides an atom-specific measure of the bonding character of states in a given energy region.

### III. RESULTS AND DISCUSSIONS

We performed a full structure search of the ternary composition space bounded by Li-Si-H at 1 atm, 50 GPa, and 100 GPa using the AIRSS code, which enabled us to construct a ternary phase, given in Fig. 1. The compounds located on the convex hull are thermodynamically stable when their enthalpy of formation is negative relative to the elements and any other compound. The ternary phase diagram is determined using the convex hull construction. From the ternary phase diagram in Fig. 1, we have identified several different stable and metastable stoichiometries, including  $\text{LiSiH}_5$ ,  $\text{Li}_2\text{SiH}_6$ ,  $\text{Li}_2\text{SiH}_{10}$ , and  $\text{Li}_2\text{SiH}_{6+\delta}$ ,  $\delta = 4, 6, 8$ . The crystal structures of these Li-Si-H compounds are shown in Fig. 2, and their structural parameters and atomic coordinates are listed in Table S1 in the Supplemental Material (SM) [22]. These results provide important pointers towards the search for the synthesis of ternary hydrogen-rich metal hydrides.

As shown in Fig. 1, there are no stable ternary compounds located on the convex hull at 1 atm. It is interesting that  $\text{LiSiH}_5$ ,  $\text{Li}_2\text{SiH}_6$ , and  $\text{Li}_2\text{SiH}_{10}$ , denoted as large solid blue circles, appear on the convex hull in our calculations at 50 and 100 GPa, indicating these ternary hydrides can be stabilized by increased pressure. In addition, the enthalpies of formation of  $\text{Li}_3\text{SiH}_{10}$ ,  $\text{Li}_2\text{SiH}_{12}$ , and  $\text{Li}_2\text{SiH}_{14}$  are less than 2 meV/atom above the convex hull at 50 or 100 GPa, and thus these compounds

are assumed to be potentially metastable. We also performed variable-composition predictions at 200 GPa, but all ternary compounds move off the convex hull, by more than 0.3 eV/atom, as shown in Fig. S1 in the SM [22]. So, below we confine our discussion to the structure and properties of the predicted stable and metastable compounds below 200 GPa.

For the stoichiometry  $\text{LiSiH}_5$ , we obtain two thermodynamically stable structures in space groups  $P2_1c$  and  $P2_12_12$  with folded layer-type  $\text{SiH}_5^-$  ions (Fig. S2 in the SM [22]). Our phonon calculations, however, show that there are too many imaginary frequencies across the whole Brillouin zone suggesting they are dynamically unstable (Fig. S3 in the SM [22]). We identify a metastable structure with space group  $R32$  which has an enthalpy just slightly higher than that of the  $P2_1c$  and  $P2_12_12$  phases, and is dynamically stable over the pressure range of 60–150 GPa (Figs. S4 and S5 in the SM [22]). This structure contains flat layer-type  $\text{SiH}_5^-$  ions, with Li atoms filling in Si-H layers [Fig. S6(b) in the SM [22]]. This is a configuration found as an inorganic structure, and is different from the  $\text{SiH}_5^-$  previously identified in  $\text{EtSiH}$  through the chemical reaction of  $\text{Et}_3\text{SiH}_2^- + \text{SiH}_4 \rightarrow \text{SiH}_5^- + \text{Et}_3\text{SiH}$  in earlier studies [23]. The only hypervalent all-hydride species reported before is the  $\text{SiH}_5^-$  ion, which was identified by mass spectrometry [24] as a product of the gas-phase ion-molecule reaction. That form of the  $\text{SiH}_5^-$  ion has been reported to be stable with respect to the loss of  $\text{H}^-$ , but unstable with respect to decomposition into  $\text{SiH}_3^-$  and  $\text{H}_2$  [25–27].  $\text{SiH}_5^-$  in  $\text{EtSiH}_5$  is composed of one axial H-Si-H unit with three H ligands perpendicular to the axial H-Si-H [26]. For the  $R32$ -type  $\text{LiSiH}_5$ , the upper Si-H layer moves  $\frac{2}{3}d_{\text{Si-H}}$  from the lower layers in the crystallographic direction [210] in  $R32$ -type  $\text{LiSiH}_5$  such that  $d_{\text{Si-H}}$  is the distance between the central Si to the H on the  $6c$  site (H on the Si-H plane), and the  $R32$  phase conforms to the  $3c-4e$  model with four H-Si-H units per central Si atom [Figs. S6(a) and S6(b) in the SM [22]]. One H-Si-H is axial and the others lie on the Si-H plane. We can assume that this layer-type  $\text{SiH}_5^-$  is composed of single  $\text{EtSiH}_5$ -type  $\text{SiH}_5^-$  ions in the  $R32$ -type  $\text{LiSiH}_5$ , and Li atoms are filled between Si-H layers. We should note that the  $3c-4e$  model does not explain why Si atoms can accommodate significant ligands in their valence shell, although it accounts for the bonding in hypervalent species.

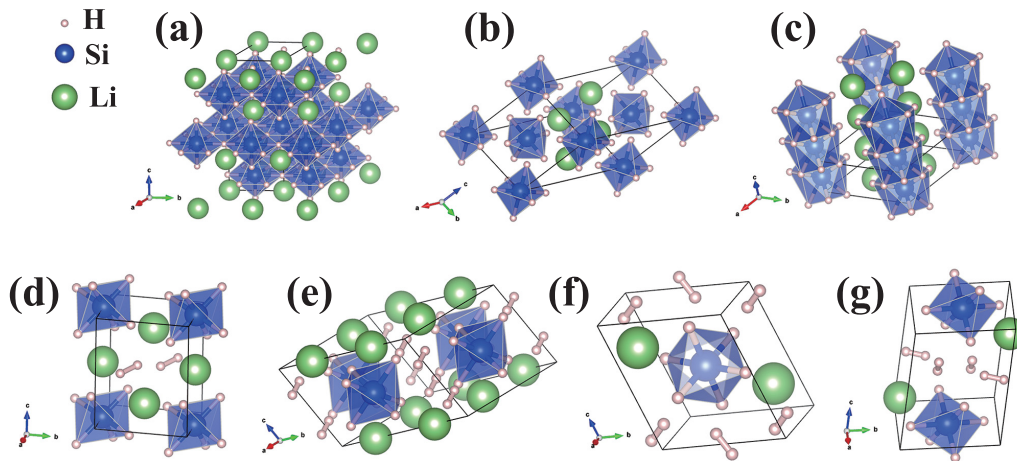


FIG. 2. Crystal structures of Li-Si-H ternary compounds, which are (a)  $R32\_LiSiH_5$  at 100 GPa, (b)  $P2_1c\_Li_2SiH_6$  at 50 GPa, (c)  $P\bar{6}2m\_Li_2SiH_6$  at 1 atm, and (d)–(g) are  $P\bar{1}\_Li_3SiH_{10}$ ,  $C2/m\_Li_2SiH_{10}$ ,  $P\bar{1}\_Li_2SiH_{12}$ , and  $P\bar{1}\_Li_2SiH_{14}$ , respectively, at 100 GPa. There is one type of  $SiH_5^-$  in the layers, and two types of  $SiH_6^{2-}$ , which are originally octahedral ions or tricapped triangular prismatic ions.

The stoichiometry  $Li_2SiH_6$  adopts the structure  $P2_1c$  at low pressure, which transforms into a  $P\bar{6}2m$  phase at 110 GPa (Fig. S7 in the SM [22]). For  $P2_1c$ -type  $Li_2SiH_6$ , the original hypervalent octahedral structure  $SiH_6^{2-}$  is favored, obeying the 3c-4e model. We have identified another tricapped triangular prismatic  $SiH_6^{2-}$  in the  $P\bar{6}2m$ -type  $Li_2SiH_6$ . There are three H atoms surrounding each Si atom lying parallel to the crystal face (001) with  $120^\circ$  angles, in a planar triangular configuration. Two Si atoms are connected by three more H atoms forming a Si-H triangular prism. Si atoms expand three unique H atoms, and share six H atoms with neighboring Si atoms to form tricapped triangular prismatic  $SiH_6^{2-}$  ions. Li atoms are filled in line in  $P\bar{6}2m$ -type  $Li_2SiH_6$ . Finally, we calculated the phonon spectra of  $P2_1c$  and  $P\bar{6}2m$  phases at different pressures, as shown in Fig. 3 and Fig. S8 in the SM [22]. The absence of phonons lying at imaginary frequencies in the phonon spectra indicates that the  $P2_1c$ -type  $Li_2SiH_6$  is dynamically stable between 50 and 100 GPa.  $P\bar{6}2m$ -type  $Li_2SiH_6$  is dynamically stable over the pressure range 0–150 GPa (Fig. S8 in the SM [22]).

For the high hydrogen content  $Li_2SiH_{10}$ , the  $C2/m$  structure is favored and this structure contains original octahedral-structured  $SiH_6^{2-}$  units, as shown in Fig. 2(e). In this structure, Li atoms and octahedral-structured  $SiH_6^{2-}$  ions are staggered and  $H_2$  molecular units fill in the gaps. Furthermore, our phonon calculations show that  $C2/m$ -type  $Li_2SiH_{10}$  is dynamically stable over the pressure range 10–100 GPa (Fig. S9 in the SM [22]).

Additional metastable compounds that we identify comprise  $Li_3SiH_{10}$ ,  $Li_2SiH_{12}$ , and  $Li_2SiH_{14}$ , and adopt the space group  $P\bar{1}$ . These all contain original octahedral-structured  $SiH_6^{2-}$  units and  $H_2$  units. A variety of Si-H bonds oriented in different directions exist with  $H_2$  units and these are extended into different directions in these structures, which reduces the symmetries of these compounds to triclinic or monoclinic. Phonon calculations show that  $Li_3SiH_{10}$  is stable at a pressure range of 70–100 GPa,  $Li_2SiH_{12}$  is stable at a pressure range of 50–100 GPa, and  $Li_2SiH_{14}$  is stable at a pressure range of 50–150 GPa (Figs. S10–S12 in the SM [22]).

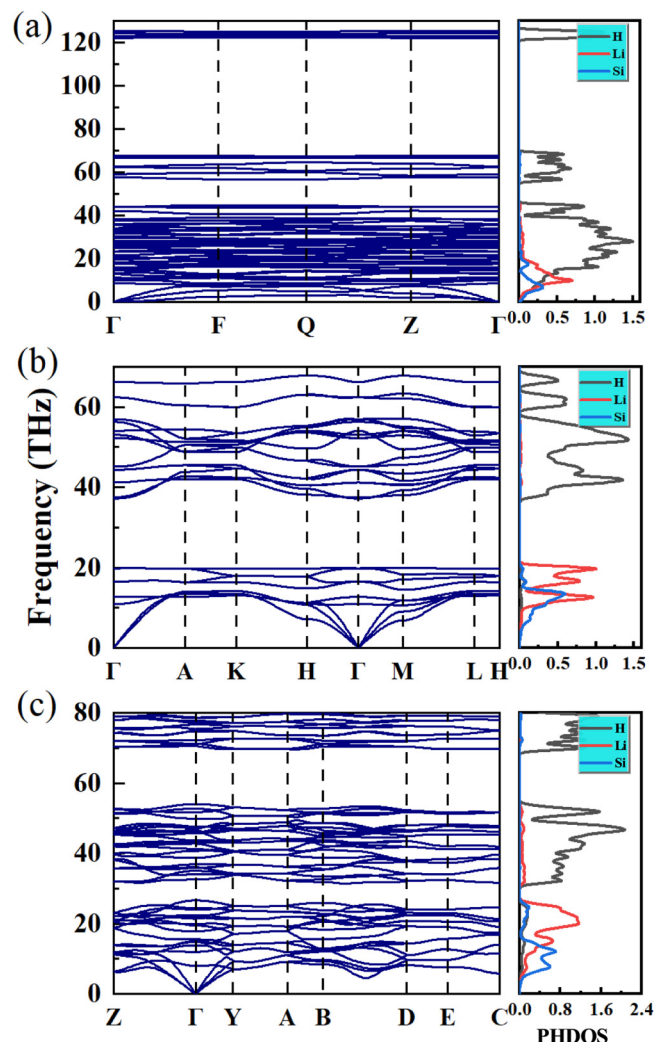
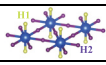
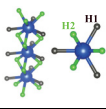
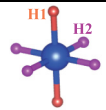


FIG. 3. Calculated phonon dispersion relations (left panel) and densities of the phonon states (right panel) of (a)  $R32\_LiSiH_5$ , (b)  $P\bar{6}2m\_Li_2SiH_6$ , and (c)  $C2/m\_Li_2SiH_{10}$  at 100 GPa.

TABLE I. The ICOHPs for Si-H bonding in  $\text{LiSiH}_5$ ,  $\text{Li}_2\text{SiH}_6$ , and  $\text{Li}_2\text{SiH}_{10}$  at different pressures.

Hydrides	Pressure (GPa)	Bond length ( $\text{\AA}$ )	ICOHP (eV)	Bonding types
$\text{LiSiH}_5$ <i>R32</i>	100	1.46	-1.97	
		1.62	-2.07	
$\text{Li}_2\text{SiH}_6$ <i>P6̄2m</i>	50	1.75	-1.19	
		1.79	-0.44	
	100	1.62	-1.65	
$\text{Li}_2\text{SiH}_{10}$ <i>C2/m</i>	50	1.51	-1.52	
		1.53	-2.73	
	100	1.46	-2.06	
		1.49	-3.01	

We have examined the electronic properties of our Li-Si-H compounds based on their equilibrium crystal structures. The Bader charge analysis [28] was used to determine charge transfer, and the electron localization function (ELF) [29] was used to describe and visualize chemical bonds in molecules and solids. A Bader charge analysis reveals a charge transfer from Li/Si to H, as listed in Table S2 in the SM [22], suggesting that both Li and Si are electron donors and provide electrons to H atoms. For all the stable phases, Li consistently loses approximately 0.8–0.9e, and Li ions form ionic bonds with Si-H anions. Furthermore, from the ELF in Fig. S13, we confirm the ionic bonding nature of Li ions in view of the absence of charge localization between Li and other elements, and weak covalent Si-H bonding via the observation of charge localization between the nearest-neighbor Si and H atoms. Moreover, in *C2/m*-type  $\text{Li}_2\text{SiH}_{10}$ , there are a lot of  $\text{H}_2$  molecular units, which is evident by the strong charge localization between the nearest-neighbor H atoms.

The electronic band structures and projected density of states (DOS) for the predicted stable and metastable structures have also been explored and are presented in Fig. 4 and Figs. S14–S18 in the SM [22]. One can see that most of the Li-Si-H compounds have large band gaps, greater than 1.0 eV, indicating that the majority of these Li-Si-H compounds are insulators except for *P1̄*-type  $\text{Li}_3\text{SiH}_{10}$ . There are few bands across the Fermi level and the values of DOS at the Fermi level are small for *P1̄*-type  $\text{Li}_3\text{SiH}_{10}$ , suggesting it is a poor electrical conductor, as shown in Fig. S18 in the SM [22].

We here propose a generally useful system to designate the bonding around the Si atoms. Such a bonding system is described as an *N-X-L* system [30]. *N* represents the number of total valence electrons, *X* is the central atom (Si in our case), and *L* is the number of ligand atoms. There are three different such systems which can be thus designated. The first is 10-Si-8 *R32*-type  $\text{LiSiH}_5$ , which is thus different from the 10-Si-5 seen in  $\text{EtSiH}_5$  [23]. Additionally, we identify 12-Si-9 for *P6̄2m*-type  $\text{Li}_2\text{SiH}_6$ , and 12-Si-6 for  $\text{Li}_2\text{SiH}_{6+\delta}$  and *P1̄*- $\text{Li}_3\text{SiH}_{10}$ .

As mentioned above, the bonding between the H and Si atoms is covalent, composing hypervalent silicic anions  $\text{SiH}_5^-$  or  $\text{SiH}_6^{2-}$ , which are strong and hard to disrupt at high pressure, as seen when we combine our data with the integrated crystalline orbital Hamiltonian population (ICOHP) [31] results in Table I. For various ICOHP values, stronger

Si-H bonds give larger negative values. There are two types of Si-H bonds in *R32*-type  $\text{LiSiH}_5$ : One is Si-H1 bonding in the flat layer with a distance of 1.46  $\text{\AA}$ , and the other is

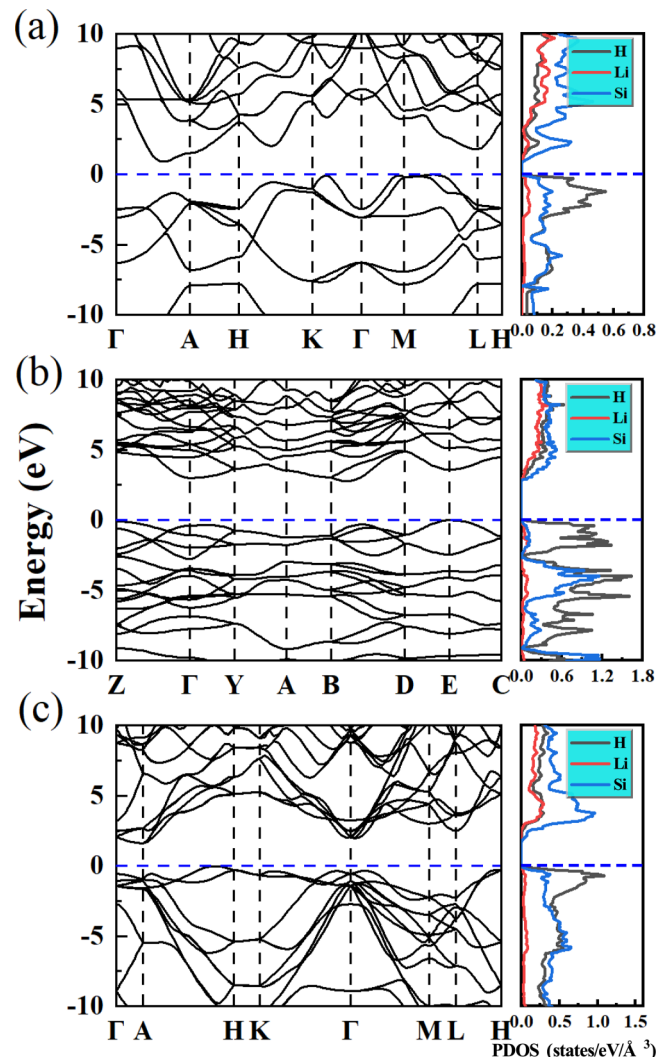


FIG. 4. Calculated band structure (left panel) and projected density of states (right panel) of (a) *R32*- $\text{LiSiH}_5$  at 100 GPa, (b) *P6̄2m*- $\text{Li}_2\text{SiH}_6$  at 1 atm, and (c) *C2/m*- $\text{Li}_2\text{SiH}_{10}$  at 10 GPa. The Fermi level is set to zero and depicted as the blue dashed line.

Si-H2 bonding perpendicular to the flat layer with a distance of 1.62 Å. The integrated ICOHP up to the Fermi levels are  $-2.08$  eV for Si-H1 bonding, and  $-1.97$  eV for Si-H2 bonding in the  $R32$ -type  $\text{LiSiH}_5$  at 100 GPa. As for  $P\bar{6}2m$ -type  $\text{Li}_2\text{SiH}_6$ , there are two types of Si-H bonding in tricapped triangular prismatic  $\text{SiH}_6^{2-}$  as well. Each of the Si atoms expands three H1 atoms involving three Si-H1 bonding with the same distance of 1.67 Å. Another interaction is Si-H2 bonding with distance of 1.62 Å, and two Si atoms are connected to three H2 atoms forming the Si-H2 triangular prism. The ICOHP up to Fermi levels are  $-1.51$  eV for Si-H1, and  $-1.65$  eV for Si-H2 at 100 GPa. For  $P2_1c$ -type  $\text{Li}_2\text{SiH}_6$ ,  $\text{Li}_2\text{SiH}_{6+\delta}$ , and  $P\bar{1}$ - $\text{Li}_3\text{SiH}_{10}$ , there is only one type of Si-H bond in the octahedral-structured  $\text{SiH}_6^{2-}$  ions. But there is a pair of Si-H bondings in longer bond lengths but more negative ICOHP values to Fermi levels. For  $C2/m$ -type  $\text{Li}_2\text{SiH}_{10}$ , a pair of Si-H1 bond lengths lie at 1.49 Å, and another two pairs of Si-H2 bond lengths are 1.46 Å at 100 GPa. It is interesting that Si-H1 with a longer bond length tends to be more stable and harder to break at high pressure. These results suggest that the Si-H bonds in anions  $\text{SiH}_5^-$  or  $\text{SiH}_6^{2-}$  are strongly covalent at high pressure and prove hard to eliminate.

It is found that all the predicted compounds have high gravimetric hydrogen contents and volumetric hydrogen densities, suggesting that they may be potential hydrogen storage materials. The  $P\bar{6}2m$ -type  $\text{Li}_2\text{SiH}_6$ , at ambient pressure, has a very high volumetric hydrogen density of 175.04 g/L with 12.51 wt % theoretical gravimetric hydrogen content. Moreover,  $P\bar{1}$ -type  $\text{Li}_2\text{SiH}_{14}$  has the highest volumetric hydrogen density of 352.31 g/L, with 25.02 wt % theoretical gravimetric hydrogen content. We plot the values of these hydrogen densities in Fig. S19 in the SM [22].

#### IV. CONCLUSIONS

In summary, we have explored the crystal structures and stabilities of compounds within the Li-Si-H ternary system

under high pressure by employing *ab initio* calculations as implemented in the AIRSS random structure search method. We predict the existences of several hydrogen-rich structures at high pressures, including  $R32$ -type  $\text{LiSiH}_5$ ,  $P\bar{6}2m$ -type  $\text{Li}_2\text{SiH}_6$ , and  $C2/m$ -type  $\text{Li}_2\text{SiH}_{10}$ . Furthermore, we find highly hydrogen-rich structures in the form of  $P\bar{1}$ -type  $\text{Li}_2\text{SiH}_{12}$ ,  $P\bar{1}$ -type  $\text{Li}_3\text{SiH}_{10}$ , and  $P\bar{1}$ -type  $\text{Li}_2\text{SiH}_{14}$ , which accommodate high hydrogen content in the form of  $\text{H}_2$  units inside. We find two different types of hypervalent ions. One of them is layer-type  $\text{SiH}_5^-$  in  $R32$ -type  $\text{LiSiH}_5$  containing four H-Si-H units per central Si atom, where one is axial and the others comprise the two-dimensional (2D) layers. The other variety of hypervalent ion that we identify is tricapped triangular prismatic  $\text{SiH}_6^{2-}$  in  $P\bar{6}2m$ -type  $\text{Li}_2\text{SiH}_6$ . This does not obey the  $3c-4e$  model and dynamically stable at both ambient pressure and high pressure. The prediction of tricapped triangular prismatic  $\text{SiH}_6^{2-}$  may be another challenge to the  $3c-4e$  model. Based on our results we propose an alternate method for designing ternary hydrogen-rich materials. We believe that our work provides useful guidance and waymarkers for future experimental synthesis of ternary alkali-metal and alkaline-earth-metal hydrides.

#### ACKNOWLEDGMENTS

This work was supported by National Natural Science Foundation of China (No. 11674122 and No. 11704143). X.F. acknowledges support via the China Scholarship Council. C.J.P. acknowledges financial support from the Engineering and Physical Sciences Research Council (Grant No. EP/P022596/1) and a Royal Society Wolfson Research Merit award. Parts of the calculations were performed in the High Performance Computing Center (HPCC) of Jilin University and TianHe-1(A) at the National Supercomputer Center in Tianjin.

- 
- [1] S. Noury, B. Silvi, and R. J. Gillespie, Chemical bonding in hypervalent molecules: Is the octet rule relevant? *Inorg. Chem.* **41**, 2164 (2002).
  - [2] P. Treichel, R. Goodrich, and S. Pierce, Synthesis and characterization of  $\text{HPF}_4$  and  $\text{H}_2\text{PF}_3$ , *J. Am. Chem. Soc.* **89**, 2017 (1967).
  - [3] R. J. Hach and R. E. Rundle, The structure of tetramethylammonium pentafluoride, *J. Am. Chem. Soc.* **73**, 4321 (1951).
  - [4] G. C. Pimentel, The bonding of trihalide and bifluoride ions by the molecular orbital method, *J. Chem. Phys.* **19**, 446 (1951).
  - [5] V. B. Koutecký and J. I. Musher, A molecular orbital description for sulfur compounds of valences 2, 4 and 6, *Theor. Chim. Acta* **33**, 227 (1974).
  - [6] G. N. Lewis, The atom and the molecule, *J. Am. Chem. Soc.* **38**, 762 (1916).
  - [7] I. Langmuir, The arrangement of electrons in atoms and molecules, *J. Am. Chem. Soc.* **41**, 868 (1919).
  - [8] R. Janot, W. Tang, D. Cléménçon, and J.-N. Chotard, Catalyzed  $\text{KSiH}_3$  as a reversible hydrogen storage material, *J. Mater. Chem. A* **4**, 19045 (2016).
  - [9] J. Chotard, W. S. Tang, P. Raybaud, and R. Janot, Potassium silanide ( $\text{KSiH}_3$ ): A reversible hydrogen storage material, *Chem. - Eur. J.* **17**, 12302 (2011).
  - [10] M. A. Ring and D. Ritter, Preparation and reactions of potassium silyl, *J. Am. Chem. Soc.* **83**, 802 (1961).
  - [11] M. A. Ring and D. Ritter, Crystal structure of potassium silyl, *J. Phys. Chem.* **65**, 182 (1961).
  - [12] K. Puhakainen, D. Benson, J. Nylén, S. Konar, E. Stoyanov, K. Leinenweber, and U. Häussermann, Hypervalent octahedral  $\text{SiH}_6^{2-}$  species from high-pressure synthesis, *Angew. Chem., Int. Ed. Engl.* **51**, 3156 (2012).
  - [13] C. J. Pickard and R. J. Needs, *Ab initio* random structure searching, *J. Phys.: Condens. Matter.* **23**, 053201 (2011).
  - [14] C. J. Pickard and R. J. Needs, High-pressure phases of silane, *Phys. Rev. Lett.* **97**, 045504 (2006).
  - [15] M. Segall, P. J. Lindan, M. A. Probert, C. J. Pickard, P. J. Hasnip, S. Clark, and M. Payne, First-principles simulation: Ideas, illustrations and the CASTEP code, *J. Phys.: Condens. Matter.* **14**, 2717 (2002).

- [16] G. Kresse and J. Furthmüller, Efficiency of *ab-initio* total energy calculations for metals and semiconductors using a plane-wave basis set, *Comput. Mater. Sci.* **6**, 15 (1996).
- [17] J. P. Perdew, K. Burke, and M. Ernzerhof, Generalized Gradient Approximation Made Simple, *Phys. Rev. Lett.* **77**, 3865 (1996).
- [18] J. P. Perdew and Y. Wang, Pair-distribution function and its coupling-constant average for the spin-polarized electron gas, *Phys. Rev. B* **46**, 12947 (1992).
- [19] P. E. Blöchl, Projector augmented-wave method, *Phys. Rev. B* **50**, 17953 (1994).
- [20] A. Togo, F. Oba, and I. Tanaka, First-principles calculations of the ferroelastic transition between rutile-type and  $\text{CaCl}_2$ -type  $\text{SiO}_2$  at high pressures, *Phys. Rev. B* **78**, 134106 (2008).
- [21] V. L. Deringer, A. L. Tchougréeff, and R. Dronskowski, Crystal orbital Hamilton population (COHP) analysis as projected from plane-wave basis sets, *J. Phys. Chem. A* **115**, 5461 (2011).
- [22] See Supplemental Material at <http://link.aps.org/supplemental/10.1103/PhysRevMaterials.4.113607> for structural parameters, phase diagram at 200 GPa, ionic diagrams, phase transition curves, phonon dispersion curves, and electronic properties of all predicted Li-Si-H compounds.
- [23] D. J. Hajdasz and R. R. Squires, Hypervalent silicon hydrides:  $\text{SiH}_5$ , *J. Am. Chem. Soc.* **108**, 3139 (1986).
- [24] J. C. Sheldon, R. N. Hayes, and J. H. Bowie, Do barriers exist for nucleophilic substitution at tetravalent silicon in the gas phase? An *ab initio* and ion cyclotron resonance study, *J. Am. Chem. Soc.* **106**, 7711 (1984).
- [25] T. Taketsugu and M. S. Gordon, Dynamic reaction path study of  $\text{SiH}_4 + \text{H}^- \rightarrow \text{SiH}_5^-$  and the Berry pseudorotation mechanism, *J. Phys. Chem.* **99**, 14597 (1995).
- [26] S. C. Pierrefixe and F. M. Bickelhaupt, Hypervalence and the delocalizing versus localizing propensities of  $\text{H}_3^-$ ,  $\text{Li}_3^-$ ,  $\text{CH}_5^-$  and  $\text{SiH}_5^-$ , *Struct. Chem.* **18**, 813 (2007).
- [27] S. C. Pierrefixe, C. Fonseca Guerra, and F. M. Bickelhaupt, Hypervalent silicon versus carbon: Ball-in-a-box model, *Chem. - Eur. J.* **14**, 819 (2008).
- [28] R. Bader, Atoms in molecules, *Acc. Chem. Res.* **18**, 9 (1985).
- [29] A. D. Becke and K. E. Edgecombe, A simple measure of electron localization in atomic and molecular systems, *J. Chem. Phys.* **92**, 5397 (1990).
- [30] C. Perkins, J. Martin, A. Arduengo, W. Lau, A. Alegria, and J. Kochi, An electrically neutral  $\sigma$ -sulfuranyl radical from the homolysis of a perester with neighboring sulfenyl sulfur: 9-S-3 species, *J. Am. Chem. Soc.* **102**, 7753 (1980).
- [31] R. Dronskowski and P. E. Blöchl, Crystal orbital Hamilton populations (COHP): Energy-resolved visualization of chemical bonding in solids based on density-functional calculations, *J. Phys. Chem.* **97**, 8617 (1993).